eLIFE elifesciences.org

RESEARCH ARTICLE

Figures and figure supplements

The cargo receptor SURF4 promotes the efficient cellular secretion of PCSK9

Brian T Emmer *et al*

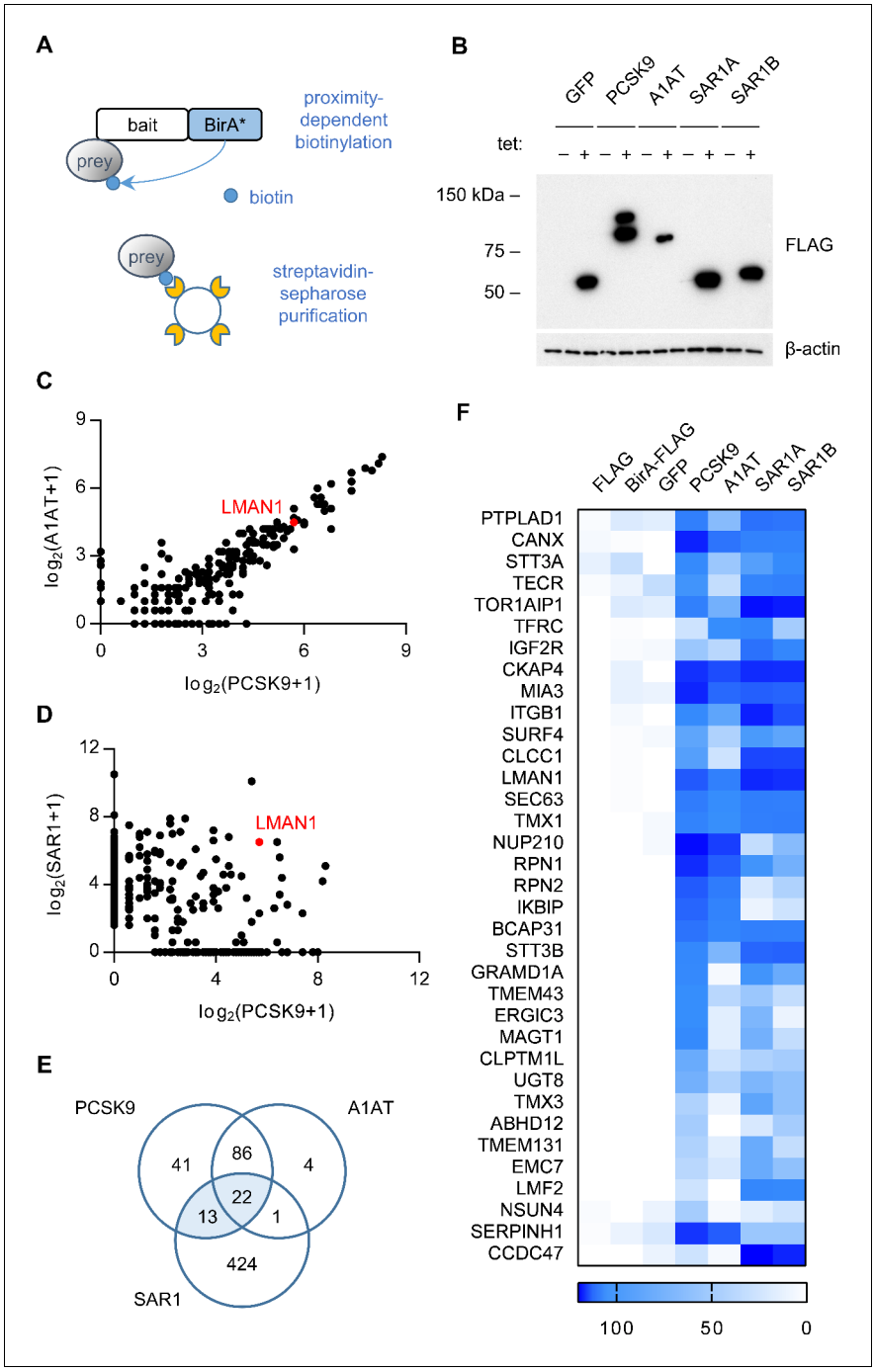

Figure 1. Proximity-dependent biotinylation with a PCSK9-BirA* fusion. (**A**) Proximity detection by mass spectrometry of streptavidin-purified prey proteins biotinylated by a fusion of BirA* to a bait protein of interest. (**B**) Immunoblotting of lysates of cells expressing various BirA*-fusion proteins. (**C**) Spectral counts of prey proteins identified from lysates of cells expressing PCSK9-BirA* relative to A1AT-BirA*. (**D**) Spectral counts of prey proteins purified from lysates of cells expressing PCSK9-BirA* relative to the maximum spectral count from lysates of cells expressing either SAR1A-BirA* or SAR1B-BirA*. (**E**) Venn diagram of identified prey proteins from lysates of cells expressing BirA* fusions with PCSK9, A1AT, or the maximum for either Sar1A or Sar1B. (**F**) Heat map of spectral counts for candidate proteins demonstrating interaction with both PCSK9-BirA* and either SAR1A-BirA* or SAR1B-BirA*. Spectral count values represent averages of 2 biologic replicates. Only prey proteins that exhibit BFDR ≤0.01 for one or more bait proteins are displayed. Source data is provided in ***Supplementary file 1***.
DOI: https://doi.org/10.7554/eLife.38839.002

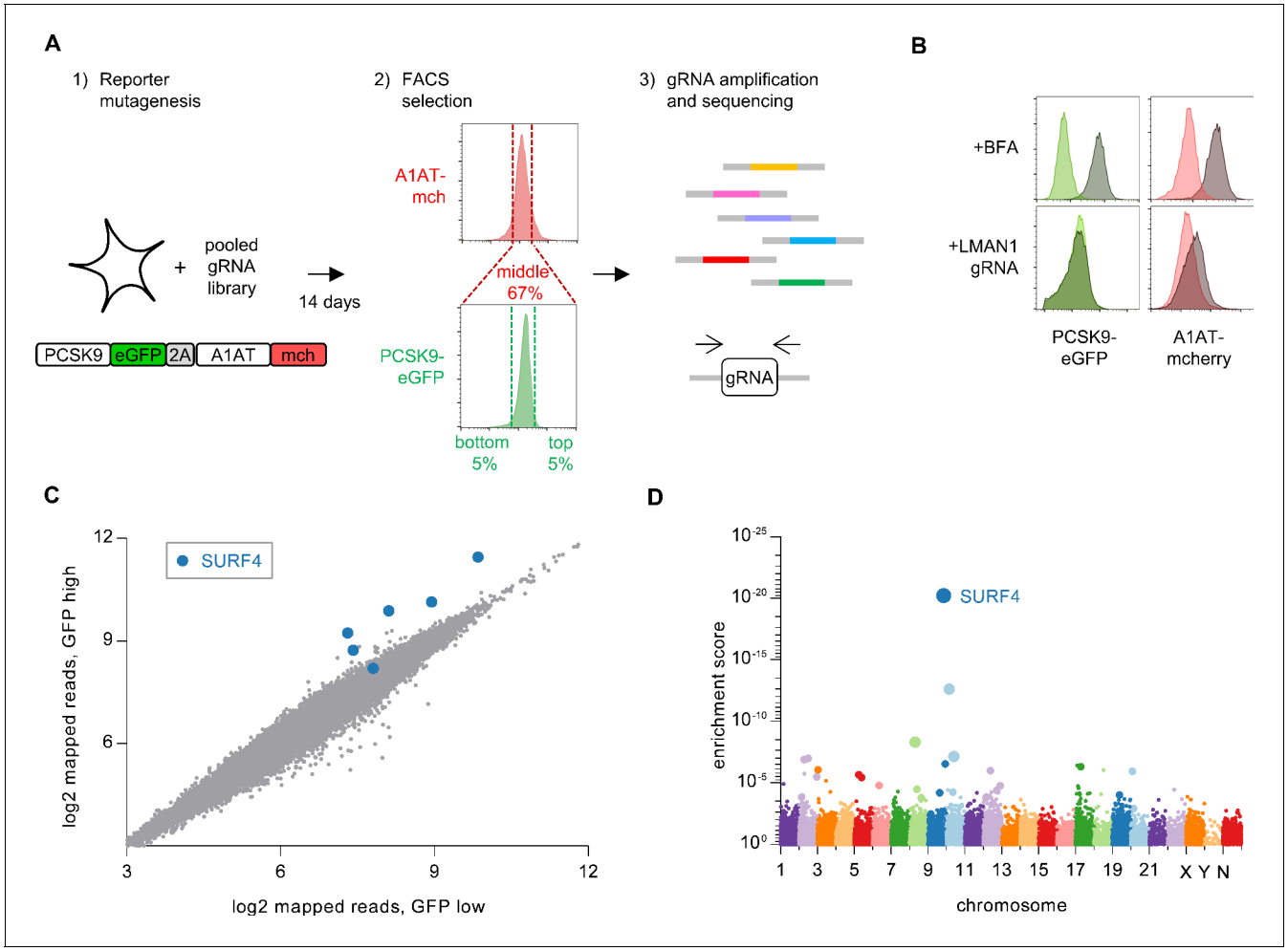

Figure 2. Whole genome CRISPR mutagenesis screen for PCSK9 secretion modifiers. (**A**) Strategy for whole genome screen. (**B**) Flow cytometry of reporter cells stably expressing PCSK9-eGFP-2A-A1AT-mCherry, treated with 1 µg/mL brefeldin A or a sgRNA targeting LMAN1. (**C**) Normalized abundance of each sgRNA in the library in eGFP high and eGFP low populations. (**D**) MAGeCK gene-level enrichment scores for each gene targeted by the library arranged by chromosome number and transcription start site. The diameter of the bubble is proportional to the number of unique sgRNAs targeting each gene that demonstrate significant enrichment in GFP high cells. Source data is provided in ***Supplementary files 2*** and ***3***.

DOI: https://doi.org/10.7554/eLife.38839.003

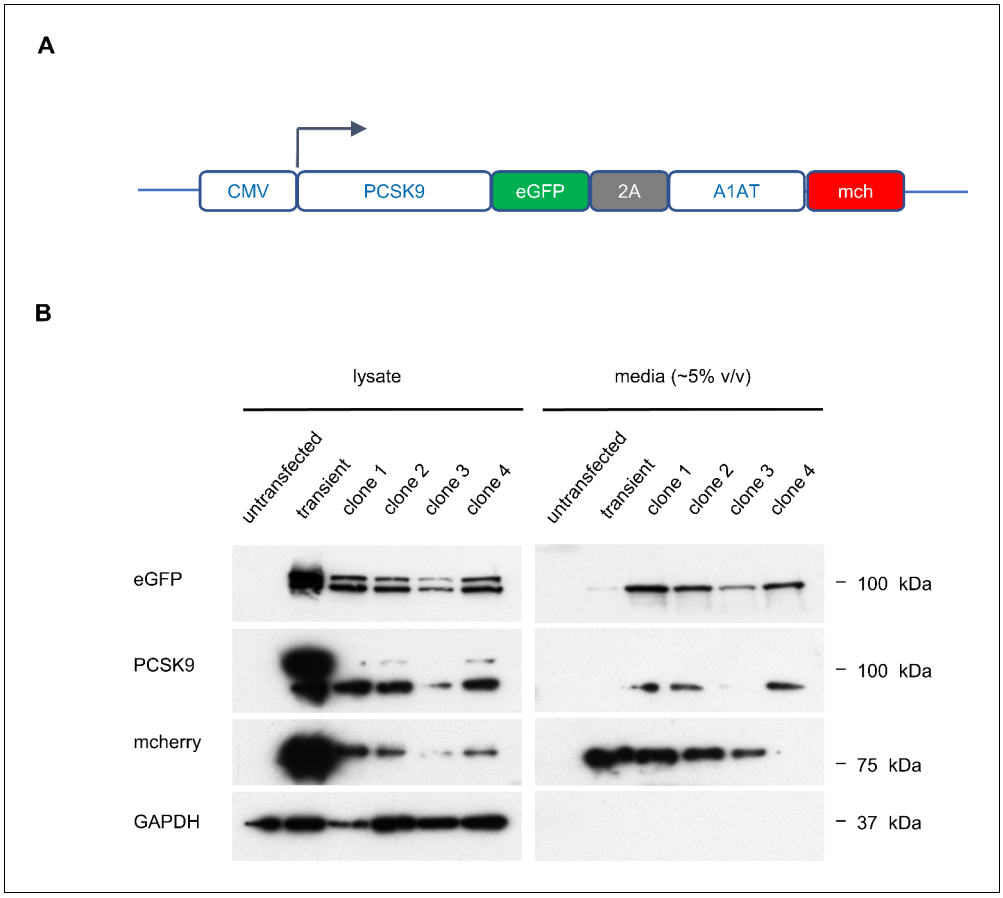

Figure 2—figure supplement 1. Analysis of PCSK9-eGFP-2A-A1AT-mCherry reporter cell clones. (**A**) Construct for CMV-promoter-driven expression of PCSK9-eGFP-2A-A1AT-mCherry expression. (**B**) Immunoblotting of HEK293T cells transfected with the PCSK9-eGFP-2A-A1AT-mCherry vector, and four individual drug-resistant clonal cell lines, relative to parental untransfected cells.

DOI: https://doi.org/10.7554/eLife.38839.004

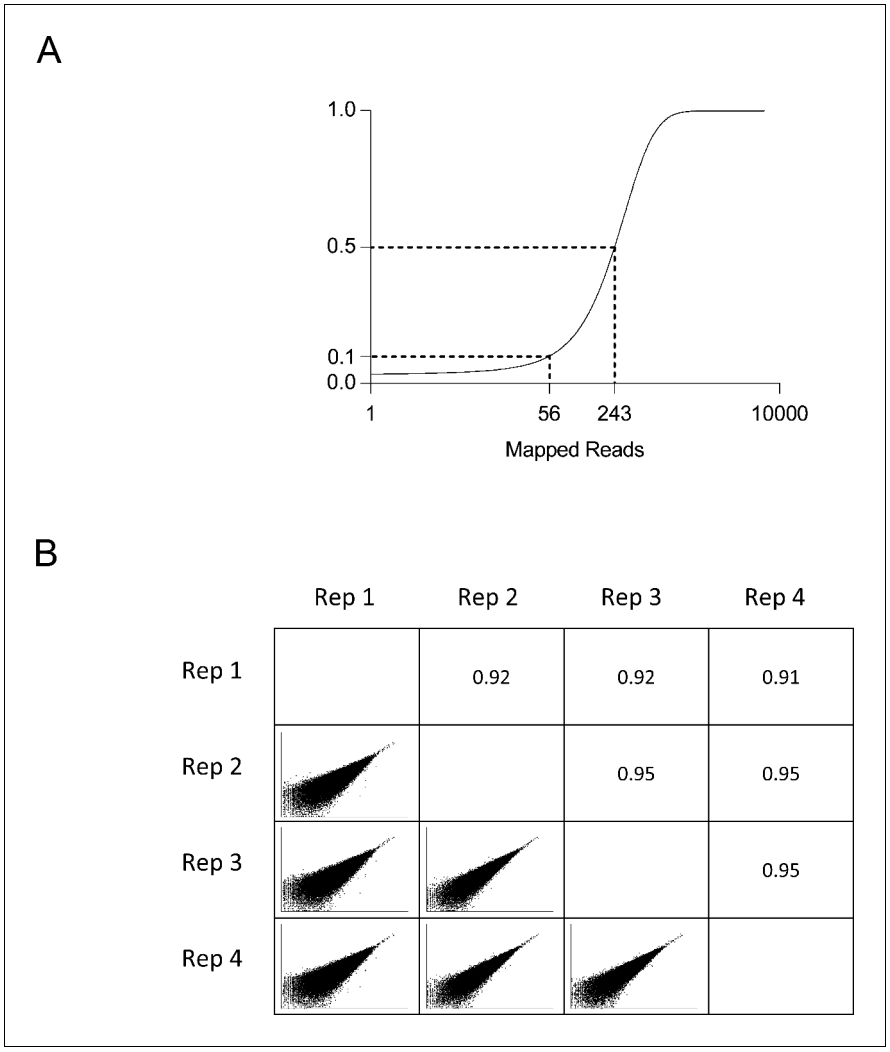

Figure 2—figure supplement 2. Whole genome screen analysis. (**A**) Cumulative distribution function of mapped reads for each sgRNA in the whole genome library. (**B**) Comparison of read counts for every pairwise combination of 4 biologic replicates with Pearson correlation coefficient.

DOI: https://doi.org/10.7554/eLife.38839.005

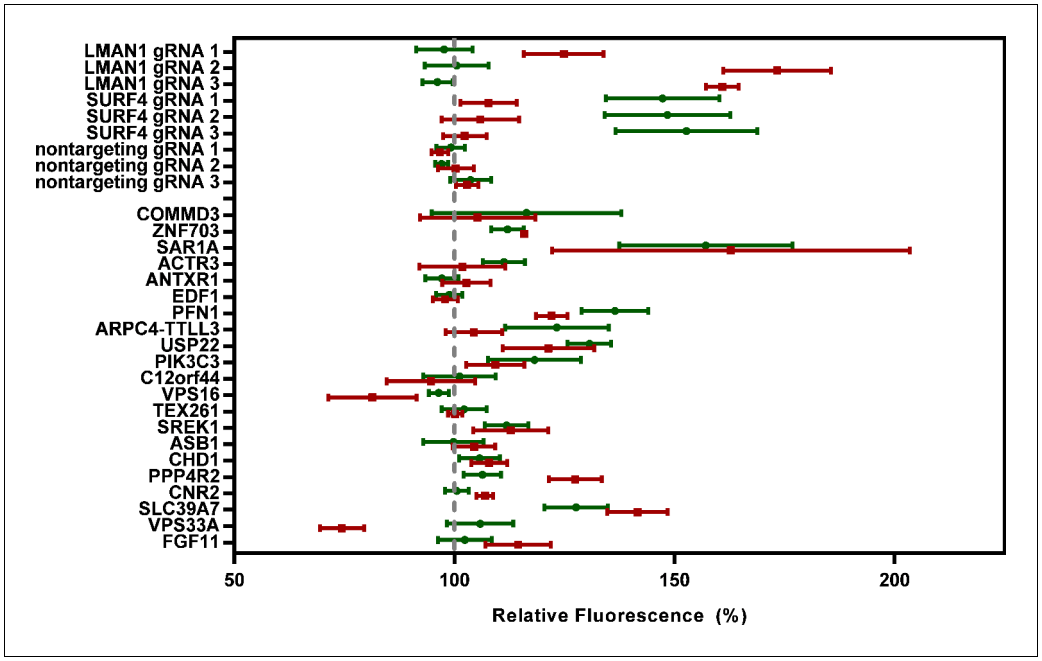

Figure 2—figure supplement 3. Validation experiments for additional candidate genes. The top-scoring sgRNA for each of the next 21 most enriched genes after *SURF4* was individually cloned into lentiCRISPRv2 and tested in PCSK9-eGFP-2A-A1AT-mCherry reporter cells. Flow cytometry was performed for each of 3 biologic replicates. The mean fluorescent intensity of PCSK9-eGFP and A1AT-mCherry for sgRNA against each candidate gene relative to nontargeting sgRNA controls is shown. Error bars represent standard deviations.
DOI: https://doi.org/10.7554/eLife.38839.006

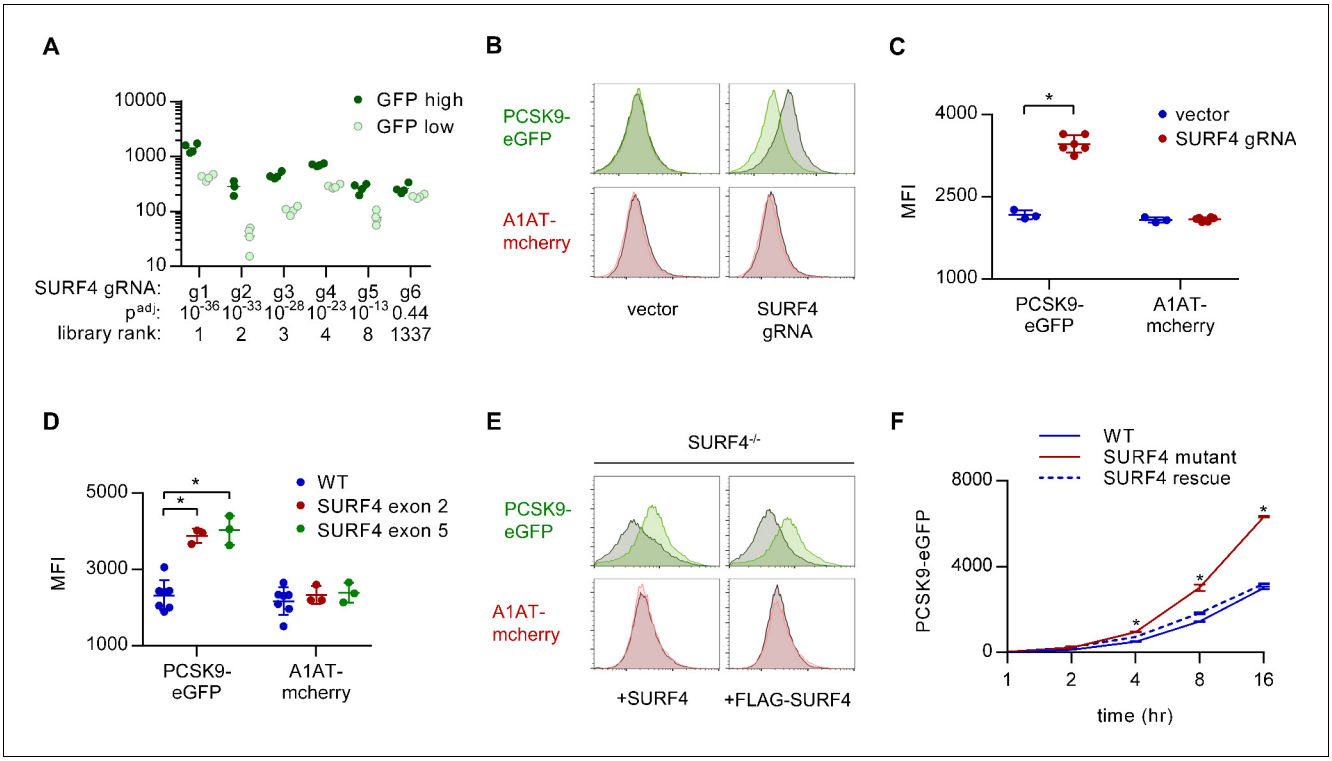

Figure 3. *SURF4* mutagenesis causes an accumulation of intracellular PCSK9-eGFP. (**A**) Individual sgRNA sequencing counts for *SURF4*-targeting sgRNA in eGFP high and eGFP low populations for each of 4 biologic replicates. Adjusted p values were calculated using DESeq2. (**B**) Flow cytometry histograms of PCSK9-eGFP and A1AT-mCherry fluorescence in reporter cells transfected with plasmids delivering Cas9 and *SURF4*-targeting sgRNA or empty vector. (**C**) Quantification of intracellular fluorescence for cells treated with empty vector (n = 3) or unique *SURF4*-targeting sgRNAs (n = 6). (**D**) Quantification of intracellular fluorescence for clonal cell lines each containing frameshift-causing indels at two different *SURF4* target sites (n = 7 wild-type clones, n = 3 clones generated from each *SURF4*-targeting sgRNA). (**E**) Flow cytometry histograms for cells expressing PCSK9-eGFP-2A-A1AT-mCherry and deleted for *SURF4* with or without stable expression of a wild-type or FLAG-tagged *SURF4* cDNA. (**F**) Time course of intracellular accumulation of tetracycline-inducible PCSK9-eGFP on WT, SURF4-deficient, or SURF4 rescue background (n = 3 biologic replicates for each cell line at each time point). *p<0.05 by Student's t-test. Error bars represent standard deviations.

DOI: https://doi.org/10.7554/eLife.38839.007

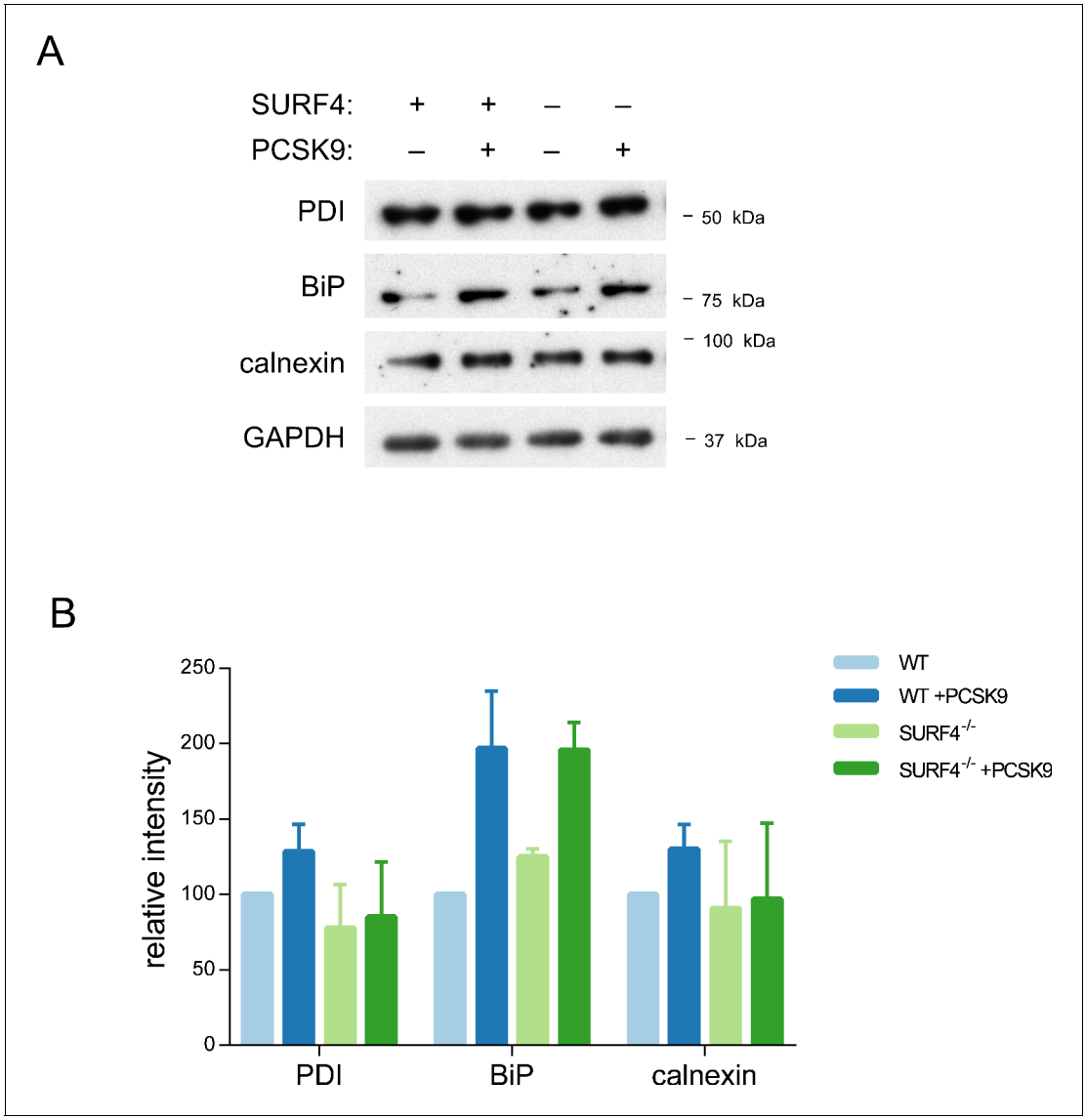

Figure 3—figure supplement 1. ER stress markers. Clonal cell lines with a stably integrated tetracycline-inducible PCSK9 cDNA on either WT or *SURF4* mutant background were treated with tetracycline or vehicle control and analyzed by immunoblotting for various markers of ER stress (**A**), quantified by densitometry (**B**). Error bars represent standard deviations.

DOI: https://doi.org/10.7554/eLife.38839.008

```
HEK293T +PCSK9-eGFP-2A-A1AT-mcherry
   clone     exon 2 WT  ACCACCT^GGAACTGCGGCTACCTGCTGG
     1         ins(1)   ACCACCTGGGAACTGCGGCTACCTGCTGG
               del(1)   ACCACC- GGAACTGCGGCTACCTGCTGG
     2         ins(1)   ACCACCTGGGAACTGCGGCTACCTGCTGG
               del(4)   ACC---- GGAACTGCGGCTACCTGCTGG
     3         ins(1)   ACCACCTGGGAACTGCGGCTACCTGCTGG
               del(6)   ACCA--- ---CTGCGGCTACCTGCTGG
              exon 5 WT  CCCAAAC^AGTACATGCAGCTCGGAGGCA
     4         ins(1)   CCCAAACAAGTACATGCAGCTCGGAGGCA
               del(1)   CCCAAAC -GTACATGCAGCTCGGAGGCA
     5         ins(1)   CCCAAACAAGTACATGCAGCTCGGAGGCA
               ins(1)   CCCAAACAAGTACATGCAGCTCGGAGGCA
     6         ins(1)   CCCAAACAAGTACATGCAGCTCGGAGGCA
               del(9)   CCCAA-- -------GCAGCTCGGAGGCA

293-TREx +PCSK9
              exon 2 WT  ACCACCT ^ GGAACTGCGGCTACCTGCTGG
     1         del(7)   ACCAC--   -----TGCGGCTACCTGCTGG
              ins(181)  ACCACCT{.}GGAACTGCGGCTACCTGCTGG
```

Figure 3—figure supplement 2. SURF4-deficient genotypes. Clonal cell lines were genotyped by PCR amplification of sgRNA target site and Sanger sequencing of the amplicon with either TIDE decomposition of individual alleles from the amplicon, or ligation of the amplicon into cloning plasmids and Sanger sequencing of multiple individual clones. Sequence corresponding to sgRNA is underlined and expected double-strand break site is indicated ().

DOI: https://doi.org/10.7554/eLife.38839.009

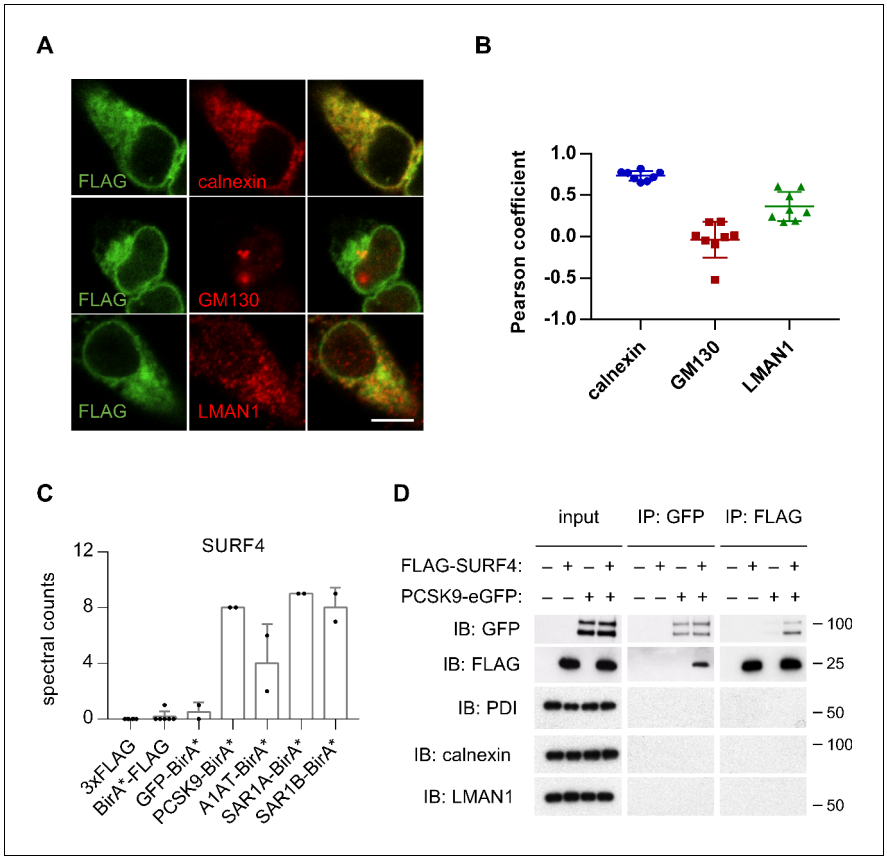

Figure 4. SURF4 localizes to the early secretory pathway where it physically interacts with PCSK9. (**A**) Immunofluorescence of FLAG-SURF4 together with markers of the ER (calnexin), ERGIC (LMAN1), and Golgi (GM130). Scale bar = 10 μm. (**B**) Quantification of colocalization (n = 8 cells analyzed for each combination of antibody staining). (**C**) Spectral counts for SURF4 in streptavidin-purified eluates from cells expressing various BirA* fusion proteins. (**D**) Immunoprecipitations were performed using antibodies directed against FLAG or GFP from lysates of cells expressing FLAG-SURF4, PCSK9-eGFP, both, or neither. Error bars represent standard deviations.
DOI: https://doi.org/10.7554/eLife.38839.010

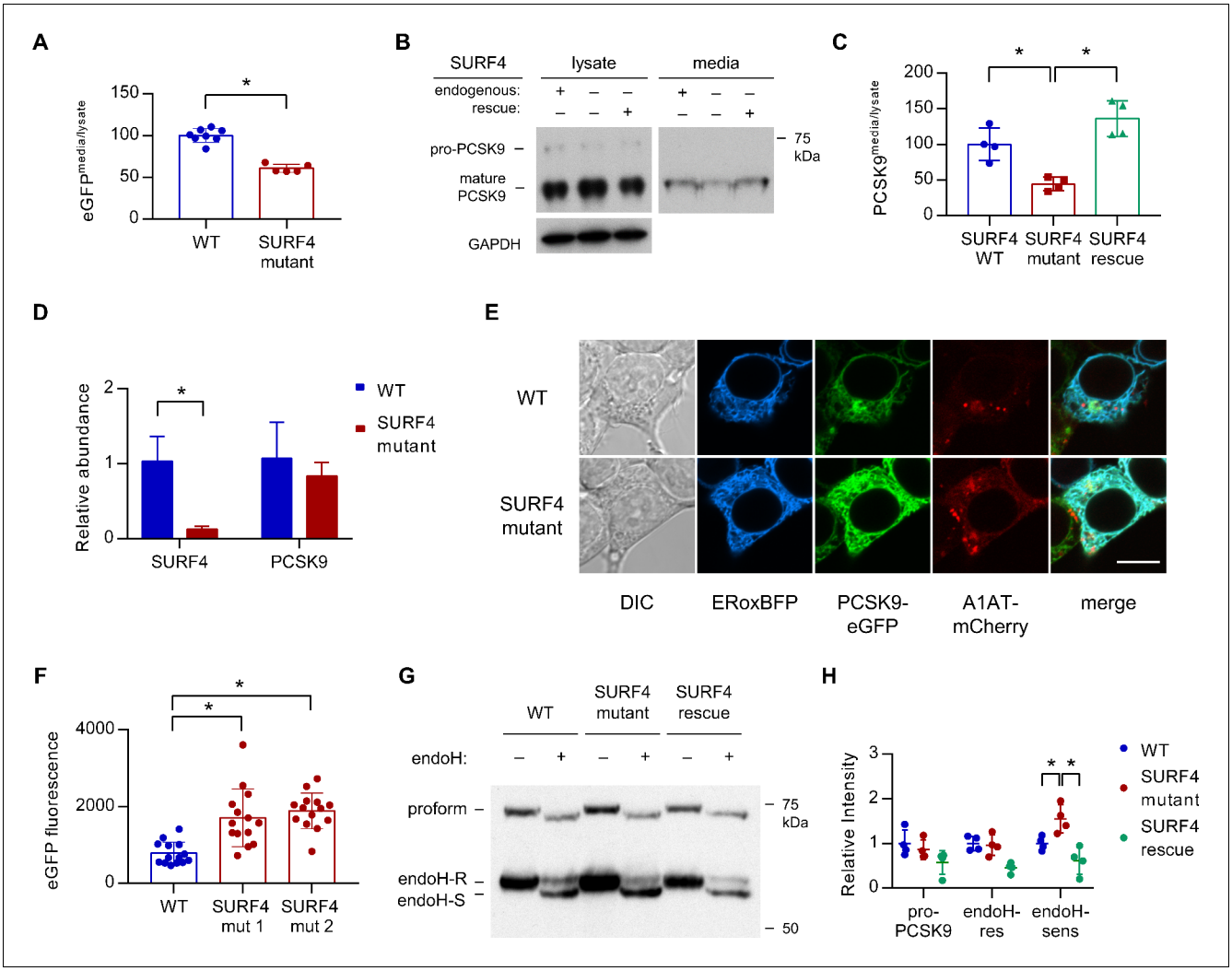

Figure 5. *SURF4* mutagenesis causes a decrease in PCSK9 extracellular secretion and an accumulation of PCSK9 in the ER. (**A**) Fluorescence detection of PCSK9-eGFP in extracellular conditioned media relative to cellular lysate in WT (n = 7) and clonal SURF4-deficient (n = 5) fluorescent reporter cell lines. (**B**) Immunoblotting of tetracycline-inducible PCSK9 in extracellular conditioned media and cellular lysates from WT, SURF4-deficient, or SURF4 rescued cells. (**C**) Quantification of densitometry of native PCSK9 relative in conditioned media and cellular lysates, normalized to GAPDH, for WT, SURF4-deficient, or SURF4 rescued cells (n = 4 biologic replicates for each cell line). (**D**) Quantitative PCR of *SURF4* and *PCSK9* transcript levels from RNA isolated from a *SURF4* WT or mutant fluorescent reporter cell line (n = 3 measurement replicates). (**E**) Live cell fluorescence microscopy of fluorescent reporter cells, either WT or SURF4-deficient, transfected with the ER marker ERoxBFP. Scale bar = 10 μm. (**F**) Quantification of PCSK9-eGFP signal intensity in pixels positive for ERoxBFP fluorescence (n = 14 for each cell line). (**G**) EndoH-sensitivity of PCSK9 expressed in WT, SURF4-deficient, or SURF4 rescued cells. (**H**) Quantification of endoH-sensitivity, normalized to average intensity of average WT band intensity (n = 4 biologic replicates for each cell line). *p<0.05 by Student's t-test. Error bars represent standard deviations.

DOI: https://doi.org/10.7554/eLife.38839.011

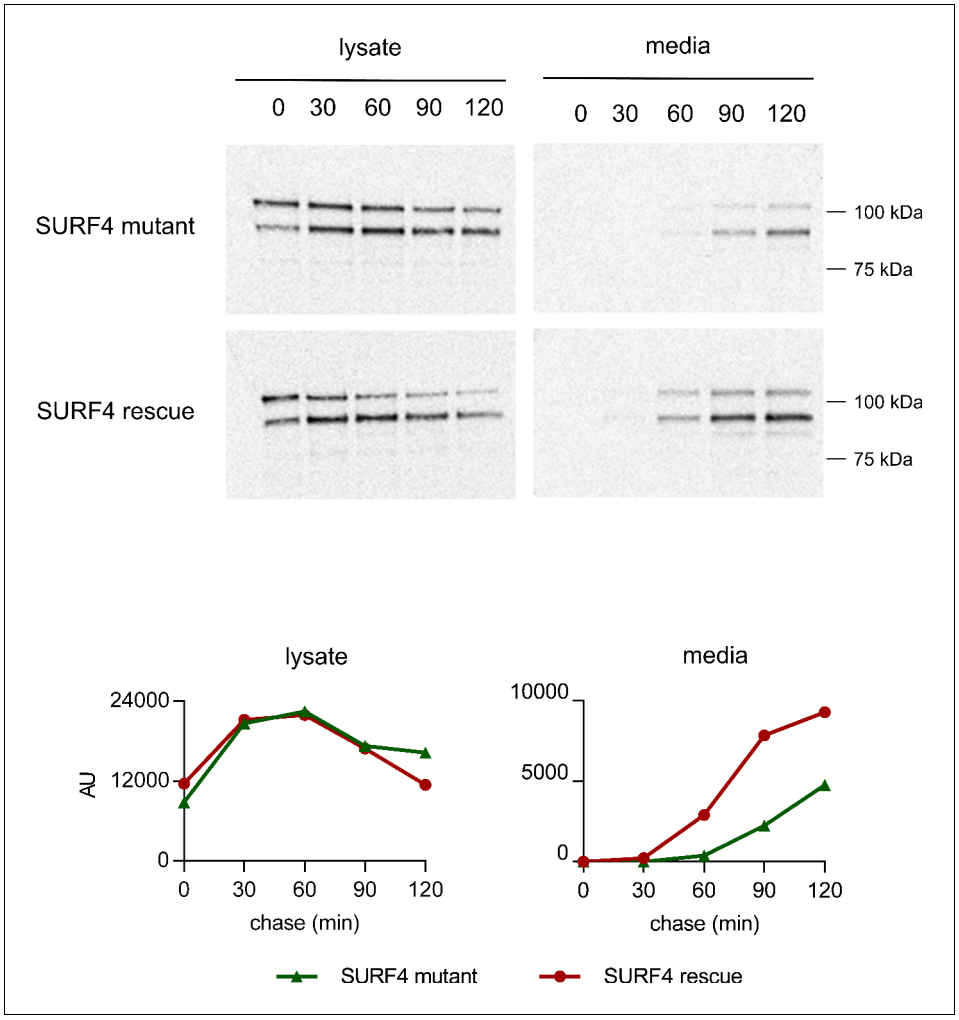

Figure 5—figure supplement 1. Pulse-chase labeling of PCSK9-eGFP secretion. A SURF4 mutant cell line with a tetracycline-inducible PCSK9-eGFP construct and with (SURF4 rescue) or without (SURF4 mutant) a stably integrated SURF4 cDNA were radiolabeled with tracer containing ^{35}S-Met and ^{35}S-Cys. Conditioned media and cellular lysates were harvested at the indicated time points and PCSK9-eGFP immunoprecipitated and analyzed by SDS-PAGE electrophoresis and autoradiography.

DOI: https://doi.org/10.7554/eLife.38839.012

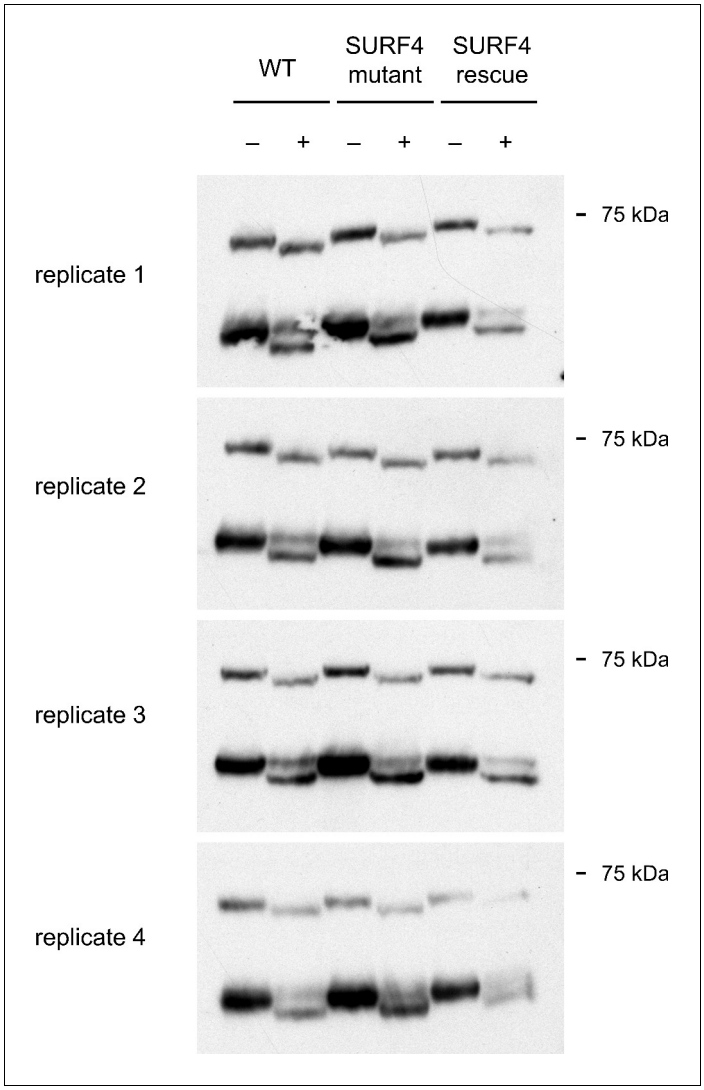

Figure 5—figure supplement 2. EndoH-sensitivity of PCSK9 expressed in WT, SURF4-deficient, or SURF4 rescued cells for each of 4 independent biologic replicates.
DOI: https://doi.org/10.7554/eLife.38839.013